Neurobiology of Aging 73 (2019) 161–170

Contents lists available at ScienceDirect

Neurobiology of Aging

journal homepage: www.elsevier.com/locate/neuaging

Lower mitochondrial DNA content but not increased mutagenesis associates with decreased base excision repair activity in brains of AD subjects

Daniela T. Soltys [a,1], Carolina P.M. Pereira [a,1], Fernanda T. Rowies [a], José M. Farfel [b], Lea T. Grinberg [b,c], Claudia K. Suemoto [d], Renata E.P. Leite [b], Roberta D. Rodriguez [e], Nolan G. Ericson [f], Jason H. Bielas [f], Nadja C. Souza-Pinto [a,*]

[a] Departamento de Bioquímica, Instituto de Química, Universidade de São Paulo, São Paulo, SP, Brazil
[b] Departamento de Patologia, Faculdade de Medicina, Universidade de São Paulo, São Paulo, SP, Brazil
[c] Department of Neurology, Memory and Aging Center, University of California, San Francisco, CA, USA
[d] Division of Geriatrics, University of São Paulo Medical School, São Paulo, SP, Brazil
[e] Department of Neurology, Behavioral and Cognitive Neurology Unit, University of São Paulo, São Paulo, SP, Brazil
[f] Division of Public Health Sciences, Fred Hutchinson Cancer Research Center, Seattle, WA, USA

ARTICLE INFO

Article history:
Received 3 April 2018
Received in revised form 13 August 2018
Accepted 13 September 2018
Available online 22 September 2018

Keywords:
Base excision repair
Alzheimer's disease
mtDNA mutation
mtDNA depletion

ABSTRACT

Accumulation of oxidative mitochondrial DNA (mtDNA) damage and impaired base excision repair (BER) in brains have been associated with Alzheimer's disease (AD). However, it is still not clear how these affect mtDNA stability, as reported levels of mtDNA mutations in AD are conflicting. Thus, we investigated whether alterations in BER correlate with mtDNA instability in AD using *postmortem* brain samples from cognitively normal AD subjects and individuals who show neuropathological features of AD, but remained cognitively normal (high-pathology control). To date, no data on DNA repair and mtDNA stability are available for these individuals. BER activities, mtDNA mutations, and mtDNA copy number were measured in the nuclear and mitochondrial extracts. Significantly lower uracil DNA glycosylase activity was detected in nuclear and mitochondrial extracts from AD subjects, while apurinic/apyrimidinic endonuclease activity was similar in all groups. Although mtDNA mutation frequency was similar in all groups, mtDNA copy number was significantly decreased in the temporal cortex of AD brains but not of high-pathology control subjects. Our results show that lower mitochondrial uracil DNA glycosylase activity does not result in increased mutagenesis, but rather in depletion of mtDNA in early-affected brain regions during AD development.

1. Introduction

As life expectancy has increased significantly in the last century, the number of Alzheimer's diseases (AD) cases in the world raised sharply, with an associated increase in public health costs. AD is characterized by progressive cognitive impairment, mostly memory, and impairment of behavioral abilities. Synaptic dysfunction and neuronal death in brain regions responsible for learning and memory are associated with the presence of amyloid plaques—extracellular deposits of amyloid beta peptide (Aβ)—and neurofibrillary tangles (NFTs) of hyperphosphorylated tau aggregates (Mattson, 2004). Despite major recent advances in identifying genes and cellular targets involved in AD pathophysiology, the molecular mechanisms leading to functional and histological changes in patients have not been fully elucidated. Several lines of evidence suggest that accumulation of oxidative DNA lesions (Krishnan et al., 2012; Wang et al., 2005) and DNA repair defects (Canugovi et al., 2014; Krishnan et al., 2012; Weissman et al., 2007) may have a role in AD progression.

Oxidized lesions are repaired, primarily, by the base excision repair (BER) pathway. Mechanistically, the BER pathway is carried out in five distinct enzymatic steps [reviewed in (Robertson et al., 2009; Wilson and Bohr, 2007)]. BER is initiated by the (1) recognition of the damaged base by a DNA glycosylase, followed by the (2) incision of the DNA backbone by apurinic/apyrimidinic (AP)

* Corresponding author at: Department of Biochemistry, Institute of Chemistry, University of Sao Paulo, Av. Prof. Lineu Prestes, 748, Bloco 10S, sala 1065, Cidade Universitária, São Paulo, SP 05508-000, Brazil. Tel.: +55 11 3091 1387; fax: +55 11 3091 2186.
E-mail address: nadja@iq.usp.br (N.C. Souza-Pinto).
[1] These authors contributed equally to this work.

0197-4580/$ – see front matter © 2018 Elsevier Inc. All rights reserved.
https://doi.org/10.1016/j.neurobiolaging.2018.09.015

endonuclease (APE1) or by the intrinsic AP-lyase activity of some DNA glycosylases. Incision of the abasic site creates single-nucleotide gaps with different 5′ or 3′ termini, which are then (3) processed by DNA polymerase β or APE1 to generate 3′-OH and/or 5′-phosphate termini, allowing (4) nucleotide incorporation by DNA polymerase. The synthesis step may proceed either via single-patch BER or long-patch BER. Single-patch BER is characterized by the incorporation of only one nucleotide, whereas in long-patch BER, there is incorporation of multiple nucleotides (2-7 nucleotides), creating a flap that is processed by Flap endonuclease 1. Finally, (v) the nick is sealed by DNA ligase.

Assessment of BER in AD brains detected lower activities in total, nuclear, and mitochondrial lysates in the cortex and cerebellum (CE) (Canugovi et al., 2014; Iida et al., 2002; Lovell et al., 2000; Weissman et al., 2007), leading to the hypothesis that lower BER sensitizes neurons to cell death induced by amyloid plaques and NFTs. However, results in mitochondria were obtained only for the inferior parietal lobe. Thus, to establish a causal relationship, more studies are needed to verify BER status in early affected brain regions related with the pathophysiology of the disease. Moreover, it is still unclear whether lower mitochondrial BER leads to mutation accumulation in mitochondrial DNA (mtDNA), as results in the literature are conflicting regarding mtDNA mutation levels in AD (Chang et al., 2000; Chinnery et al., 2001; Coskun et al., 2004; Hoekstra et al., 2016; Lin et al., 2002).

Thus, we analyzed BER activity, mtDNA mutation frequency, and copy number in two brain regions, temporal cortex (TC) and CE, as the former is an early affected region for plaques and tangles, respectively, and the latter accumulates plaques only in late stages of AD (Braak and Braak, 1991; Montine et al., 2012; Thompson et al., 2003). The analyses were performed in postmortem brains from three groups: normal, AD, and high-pathology control (hpC) subjects, individuals who meet criteria to high AD neuropathologic changes (ADNCs) (Montine et al., 2012), but remained cognitively normal. This third group is important to investigate the molecular mechanisms that protect the brain against accumulation of DNA damage and prevent the development of cognitive impairment and to ascertain whether changes in the parameters tested are causal or resulted from the accumulation of plaques and tangles, regardless of the development of the disease.

2. Materials and methods

2.1. Experimental groups

Three groups were used in this study: (1) control (C), cognitively normal without AD neuropathology; (2) hpC, cognitively normal with high ADNC; and (3) AD with moderate or severe dementia and high ADNC. Postmortem brain samples were obtained from the Brazilian Aging Brain Study Group's Brain Bank, University of São Paulo School of Medicine. The samples were collected through the City of São Paulo Death Verification Service, after obtaining informed consent from family members. Cognitive screening was performed by the Informant Questionnaire on Cognitive Decline in the Elderly —retrospective version (Jorm and Jacomb, 1989) and the Clinical Dementia Rating (Morris, 1993) applied to the subject's family. The distribution and localization of amyloid plaques and NFTs were analyzed according to Consortium to Establish a Registry for Alzheimer's Disease (CERAD) score (Mirra et al., 1991) and Braak stage (Braak and Braak, 1991), respectively. The subjects were scored according to cognitive (Clinical Dementia Rating and Informant Questionnaire on Cognitive Decline in the Elderly) and neuropathological (CERAD score and Braak stage) criteria and classified into the three groups (Table 1). The groups were paired for age and followed the inclusion criteria described in the study by Grinberg et al., 2007.

Table 1
Classification of experimental groups by clinical and pathological criteria

Groups	CDR	IQCODE	CERAD	Braak staging
Control (C)	0	<3,20	0 or A	≤ III
High-pathology control (hpC)	0	<3,20	B or C	≥ IV
Alzheimer's disease (AD)	≥2	>3,80	B or C	≥ IV

CDR scale and IQCODE clinical functional assessments used for cognitive classification; CERAD criteria and Braak staging—neuropathological assessment of AD pathology.
Key: CDR, clinical dementia rating; IQCODE, informant questionnaire on cognitive decline in the elderly.

2.2. Preparation of nuclear and mitochondrial extracts

Nuclear and mitochondrial fractions were isolated from 0.5 to 1 g of frozen CE or TC as described (Karahalil et al., 2002; Soltys et al., 2015), using Ficoll 400 gradient to separate mitochondrial fractions. Protein extracts were obtained by suspending the fractions in the buffer containing 20 mM HEPES (pH 7.0), 150 mM KCl, 2 mM EDTA, 1% Triton X-100, and protease inhibitors (Roche, Basel, Switzerland), incubated for 1 hour, at 4 °C with shaking and centrifuged at 50,000 × *g* for 1 hour. Supernatants were collected, and glycerol was added to a final concentration of 10%. All steps were performed at 4 °C. Protein concentration was measured by Bradford (Bradford, 1976), using bovine gamma globulin as standard (Bio-Rad Laboratories Inc, Hercules, CA, USA).

2.3. Western blotting

Purity of the mitochondrial fractions was assessed by standard Western blot techniques using 10 μg of each fraction and antibodies against Lamin B2 (X223; 1:500) (nuclear marker) and COX4 (20E8; 1:750) (mitochondrial marker), all from Santa Cruz Biotechnology, Santa Cruz, USA. For uracil DNA glycosylase (UDG) protein levels and mitochondrial content, 50 μg of whole-cell extracts was used with the following antibodies: UNG (K1C12; 1:500; Abcam), COX4 (6B3; 1:500; Novus Biologicals), and β-actin (ab6276; 1:10,000; Abcam).

2.4. In vitro measurement of BER activities

BER was measured using oligonucleotide incision assays with fluorescent-labeled oligonucleotides containing site-specific lesions, as described (Soltys et al., 2015). Oligonucleotides containing uracil (U), tetrahydrofuran (abasic site analog) (AP), or a non-modified base (Ctrl) at position 11 were used in this study. The substrates were obtained commercially (U, Ctrl, and complementary strands from Invitrogen, Life Technologies, Carlsbad, CA, USA; AP from Midland Certified Reagent Company, Midland, TX, USA). Supplementary Fig. 1 shows the sequence of the oligonucleotides and a schematic representation of the incision assay. In vitro assays were performed as described in the study by Maynard et al., 2010, using 50 fmoles of fluorescent-labeled substrate per reaction. Recombinant APE1 and UDG were purchased from New England Biolabs (Ipswich, MA, USA) and used as positive controls. Incubation time and protein concentrations were determined experimentally for each substrate and brain region. For uracil, reactions containing 5 μg of CE nuclear or mitochondrial extracts were incubated at 37 °C for 30 minutes (nuclear) or 1 hour

(mitochondrial). For TC extracts, reactions contained 5 μg (nuclear) or 10 μg (mitochondrial) of protein extracts. For AP, reactions containing 10 ng of CE nuclear or mitochondrial extracts were incubated for 5 minutes (nuclear) or 10 minutes (mitochondrial), whereas 10 ng (nuclear) or 25 ng (mitochondrial) of TC protein extracts were incubated at 37 °C for 10 minutes (nuclear) or 15 minutes (mitochondrial). The products were resolved under denaturing conditions (23% acrilamida/bis-acrilamida 19:1, 7M Urea, tris-borate-EDTA [Tris base 0.22M, Boric acid 0.18M, EDTA 5 mM] 1×), visualized in the laser scanner Typhoon Trio (GE Healthcare Life Sciences, Buckinghamshire, UK) and quantified using ImageQuant (GE Healthcare Life Sciences).

2.5. Citrate synthase activity

Citrate synthase (CS) activity was measured in a 96-well microplate following the procedure described by Oroboros Instruments Company (Eigentler et al., 2015). For each reaction, 3 μg of mitochondrial or whole-cell extracts was incubated with 0.1 M Tris-HCl buffer (pH 7.1), 250 μM oxaloacetate, 100 μM DNTB, and 50 μM acetyl-coenzyme A. Absorbance at 412 nm was monitored for 5 minutes at 30 °C, and the inclination of blank or sample-containing reactions were calculated per minute. Enzyme activity, in international units (IU, mU/mL), was calculated using the molar absorptivity coefficient of TNB (13.6 $mM^{-1} \times cm^{-1}$) and optical path length for the total volume of reaction (0.527 for 0.2 mL). The data were normalized to protein concentration, and the results are presented in mU/mg of protein (nmols/min/mg of protein).

2.6. DNA extraction

Total DNA was isolated from 10 mg of postmortem brain samples using the DNeasy Blood & Tissue Kit (Qiagen, Hilden, Germany) according to the manufacturer's instructions.

The amount and quality of DNA were checked by spectrophotometry (NanoDrop, Thermo Scientific, Waltham, MA, USA) and by quantitative polymerase chain reaction (PCR) (qPCR). On qPCR reactions, 1 μL of total DNA (diluted 10× in water) was amplified with 500 nM of primers for mtDNA (Walker' primers, see Supplementary Table 1). PCRs were performed in duplicate in 25 μL reactions with GoTaq qPCR Master Mix (Promega, Fitchburg, WI, USA). Cycling and reading were performed in the CFX96 Touch Real-Time PCR Detection System (Bio-Rad Laboratories, Hercules, CA, USA) using standard thermal cycling conditions and annealing temperature of 65 °C.

2.7. Random mutation capture assay and mtDNA copy number

MtDNA mutation rate was analyzed using the random mutation capture (RMC) assay, as described (Bielas and Loeb, 2005; Valente et al., 2016; Wright et al., 2011). Total DNA (500 ng) was incubated with 10 U of TaqI enzyme (Fischer Scientific, Hampton, NH, USA) in TaqI buffer (1×) for 1 hour at 65 °C, for 20 successive rounds of digestion. The digested DNA was used in droplet digital PCR (ddPCR) reactions on the QuantaLife Droplet Digital PCR system (QuantaLife, Bio-Rad Laboratories), with mtDNA targets inside (TaqI 1216 and 8006 sites) and outside (Walker) the TaqI site. The amplification of the region outside the TaqI site was performed with 1 μL of diluted digested DNA (dilution of 500× to 2000×) and for the TaqI sites with 5 μL of nondiluted digested DNA. The digested DNA, primers, and probes were mixed with ddPCR Master Mix (Bio-Rad Laboratories) to a final reaction volume of 25 μL. Reaction droplets were made by applying 20 μL of each reaction mixture to a droplet generator DG8 cartridge in the QuantaLife Droplet Generator (QuantaLife), and cycling was performed on the MyCycler thermal cycler (Bio-Rad Laboratories) using standard conditions and an annealing temperature of 65 °C. The thermally cycled droplets were then analyzed by flow cytometry on a QuantaLife Droplet Digital PCR system (QuantaLife). The number of positive droplets was calculated automatically by the accompanying software (QuantaSoft, Bio-Rad Laboratories) using Poisson statistics, as described elsewhere (Hindson et al., 2011). mtDNA copy number was measured as the relative amplification ratio between mitochondrial (Walker) and nuclear (RPP30) loci, using ddPCR assays performed with TaqI-digested DNA and the appropriate primers/probe sets. Supplementary Table 1 shows sequence and targets for primers/probe set.

2.8. Statistical analysis

All assays were performed in duplicate with at least two independent experiments, and the results were plotted as mean ± standard deviation.

Data from each group were analyzed by Grubb's test for possible outliers. Normality and the equality of variances were analyzed by Shapiro-Wilk test and Levene's test, respectively. For normal distribution data, the one-way ANOVA with Tukey's post hoc test was used. Otherwise, the Kruskal-Wallis with Mann-Whitney post hoc test was used. All analyses were carried out by the Prism GraphPad version 5.01 software (GraphPad Software, La Jolla, CA, EUA) and SigmaStat version 3.5 (Systat Software, Chicago, IL, EUA). Differences between experimental groups were considered significant when $p<0.05$.

3. Results

3.1. Characterization of experimental groups

The demographic, clinical, and pathological data of individuals included in this study are presented in Table 2. Only samples with postmortem interval inferior to 24 hours were used, as previous results from our group showed that BER activities were preserved in rat brains up to 24 hours after death (Soltys et al., 2015).

Variation in age and education between the groups were analyzed by one-way ANOVA and Tukey's post hoc tests and showed no significant differences between the three groups for both parameters. Some individuals included in the hpC group displayed histopathological features not only of AD but also of other dementia, such as Parkinson's disease and vascular dementia, while still preserving cognition, indicating that they are also protected from the clinical outcomes of the neuropathological features characteristic of these diseases.

3.2. Nuclear and mitochondrial UDG activities are reduced in AD brains and inversely correlated with disease hallmarks

Mitochondrial and nuclear extracts from TC and CE from control, hpC, and AD individuals were assayed for BER activities using an in vitro oligonucleotide incision assay. We measured incision of a fluorescent-labeled 30-mer oligonucleotide containing a deoxyuridine at position 12, and enzyme activity was calculated from the ratio between the 18-mer product (arrow) and the uncleaved 30-mer (Supplemental Fig. 1, Fig. 1A). Recombinant UDG was used as the positive control. UDG is the main DNA glycosylase responsible for removing uracil from DNA in the nucleus and in the mitochondria (Krokan et al., 2001), thus U-incision is referred to as UDG activity. Nuclear UDG activity was significantly lower in both AD brain regions when compared with control individuals, whereas no statistically significant differences were detected in the hpC group

Table 2
Demographic, clinical, and pathological data of the individuals included in the study

Experimental groups	Subject	Age	Gender	Education (y)	Braak stage	IQ	CDR	CERAD	PMI (h)	Histopathology
Control										
	1	79	M	4	0	3	0	A	14.38	Normal
	2	80	M	4	2	3	0	0	15.38	Normal
	3	84	F	4	1	3	0	0	11.38	Normal
	4	89	F	8	2	3	0	0	5.38	Normal
	5	75	M	4	2	3	0	A	17.05	Normal
	6	74	F	0	2	3	0	A	16.28	Normal
	7	73	F	12	0	3	0	0	8.66	Normal
	8	64	F	0	2	3.04	0	0	12.18	Normal
	9	68	M	8	2	3	0	A	13.8	Normal
	10	82	M	2	2	3	0	A	14.08	Normal
	Mean ± SD	76.8 ± 7.52		4.6 ± 3.77						
Alzheimer's disease										
	1	82	M	2	6	5	3	C	15.33	AD
	2	80	M	4	5	4.73	3	C	18.6	AD
	3	83	F	2	6	4.92	3	B	12.05	AD
	4	72	M	8	6	4.46	2	C	7.78	AD
	5	81	F	1	4	5	3	B	13.66	AD
	6	79	F	4	6	5	3	C	16	AD
	7	94	F	0	6	4.8	3	C	12.31	AD
	8	81	F	0	5	4.7	2	C	13.75	AD
	9	93	F	4	6	5	3	C	10.4	AD
	10	79	F	0	6	5	3	C	14.68	AD+PD
	Mean ± SD	82.4 ± 6.57		2.5 ± 2.55						
High-pathology control										
	1	82	M	1	4	3	0	B	22.91	AD
	2	87	F	12	5	3.04	0	C	8.66	AD + VD
	3	83	F	8	4	3	0	B	20.66	AD + PD
	4	73	M	15	4	3	0	C	8.16	AD
	5	80	F	4	5	3	0	C	13.58	AD + VD
	6	80	M	4	5	3	0	C	9.41	AD
	7	95	F	4	3	3	0	B	13.41	AD
	8	81	F	4	4	3	0	C	11.3	AD+VD
	9	85	F	8	4	3	0	B	11.65	AD+PD
	10	89	F	2	4	3	0	C	13.08	AD
	Mean ± SD	83.5 ± 5.96		6.2 ± 4.49						

CDR scale and IQCODE—clinical functional assessments used for cognitive classification; CERAD criteria and Braak staging—neuropathological assessment of AD pathology.
Key: AD, Alzheimer's disease; CDR, clinical dementia rating; IQCODE, informant questionnaire on cognitive decline in the elderly; PMI, *postmortem* interval; PD, Parkinson's disease; VD, vascular dementia.

(Fig. 1B and C). Interestingly, for all groups, nuclear UDG activity was inversely correlated with CERAD score (Fig. 1D and F) and Braak stages (Fig. 1E and G) in both regions.

To measure BER in the mitochondrial compartment, we prepared highly purified brain mitochondria, as nuclear contamination could mask differences among the groups due to higher activities of nuclear BER enzymes when compared with mitochondrial extracts (Karahalil et al., 2002). Purity of mitochondrial fractions was tested measuring the presence of Lamin B2, an exclusively nuclear protein, in the extracts. COX4, an exclusively mitochondrial protein, was used as the mitochondrial marker. A representative Western blot is shown in Fig. 2A. All mitochondrial preparations used here showed less than 5% of nuclear contamination. To account for differential mitochondrial enrichment during isolation, we measured CS activity, a surrogate for mitochondrial content (Holloszy et al., 1970), which was used to normalize BER activities for each sample. CS activity did not vary among the groups in both brain regions (Fig. 2B and C), indicating similar mitochondrial enrichment during isolation.

Mitochondrial UDG activity was assayed and resolved as described, and a representative gel is shown in Fig. 2D. Mitochondrial UDG was significantly reduced in the AD group when compared with controls in TC (Fig. 2F), but not in CE (Fig. 2E). UDG activity in the hpC group was not statistically different from the control ($p = 0.2716$). TC mitochondrial UDG activity was also inversely correlated with CERAD score (Fig. 2G) and Braak stage (Fig. 2H). Importantly, mitochondrial UDG activity showed no correlation with postmortem interval for the individuals included here (Supplementary Fig. 2), in accordance with our previous results that BER activities are preserved up to 24 hours after death (Soltys et al., 2015).

As lower uracil incision activity was observed in AD nuclear and mitochondrial extracts, we quantified UDG expression in whole-brain extracts to ascertain whether UDG protein levels were decreased. However, UDG expression was similar in all three experimental groups (Supplementary Fig. 3).

3.3. Nuclear and mitochondrial APE1 activities are not altered in AD subjects

APE1 is the major abasic site (AP) endonuclease in mammalian cells and catalyzes the second enzymatic step in BER (Wilson et al., 1995). APE1 activity was measured in nuclear (Fig. 3A) and mitochondrial (Fig. 3D) extracts with a fluorescent-labeled 30-mer duplex containing the abasic site analogue tetrahydrofuran at position 12 (AP duplex). APE1 activity in nuclear (Fig. 3B and C, for CE and TC, respectively) or in mitochondrial (Fig. 3E and F, for CE and TC, respectively) extracts was similar in all three groups, indicating that AP-site incision is preserved during the AD neurodegenerative process.

3.4. mtDNA mutation frequencies are not increased in AD

It has been proposed that accumulation of mtDNA mutations and deletions drive AD pathology (Wallace, 2005). mtDNA

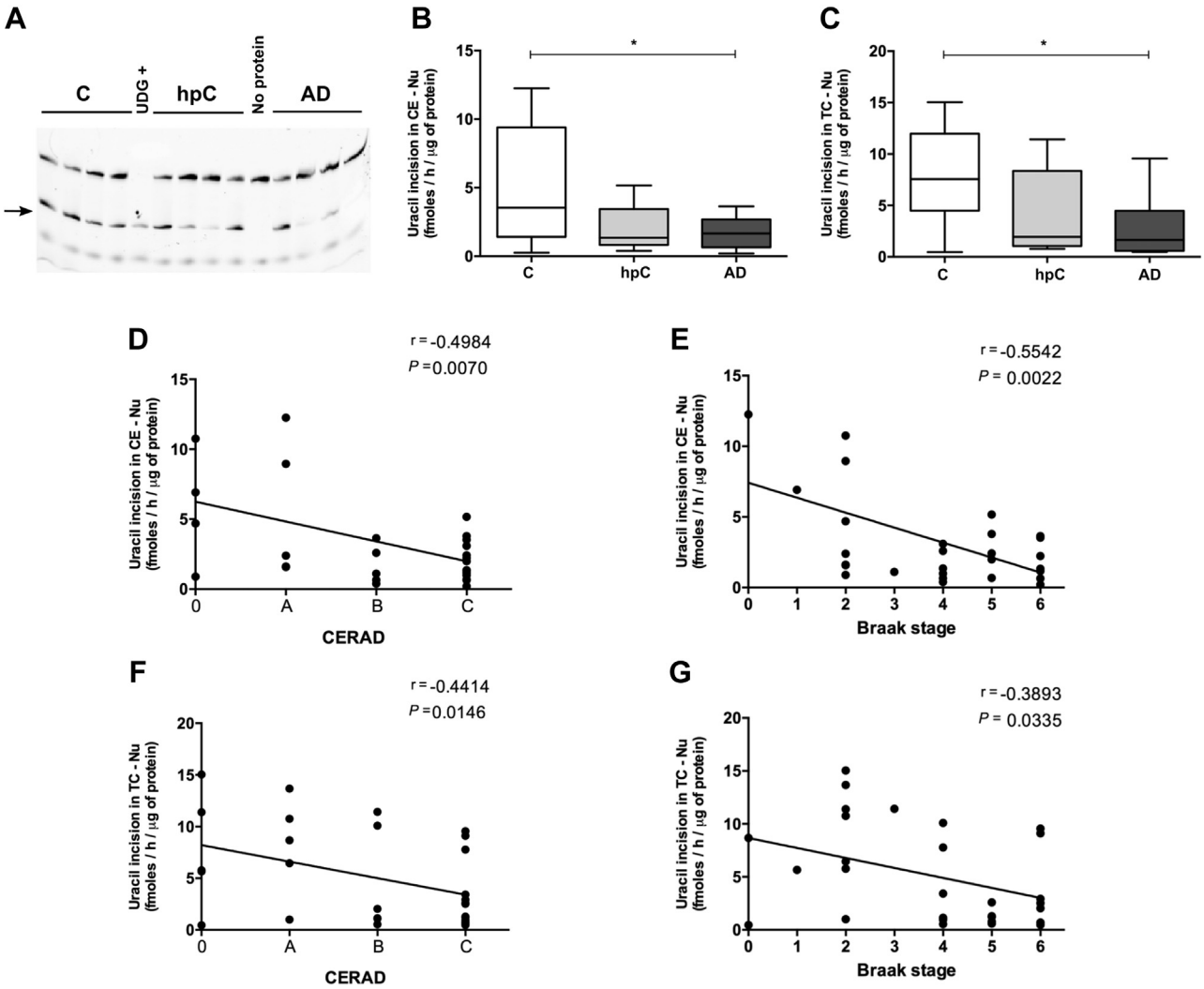

Fig. 1. Nuclear UDG activity is reduced in AD cerebellum and temporal cortex. Nuclear extracts, prepared from *postmortem* brains, were incubated with a U-containing substrate (U duplex) and resolved as described. A representative gel is presented in (A) and the migration of the product is indicated by an arrow; recombinant UDG (UDG+) was used as a positive control. Uracil incision was measured in nuclear extracts from cerebellum (CE) (B) or temporal cortex (TC) (C) of individuals described in Table 1. Uracil incision activity for each individual was plotted against CERAD score (D and F) or Braak stage (E and G). R values represent the Pearson's coefficient and p values <0.05 are considered statistically significant. The incision values presented are mean ± SD of two independent experiments, performed in duplicate (n = 10 per group). * $p < 0.05$. Abbreviations: AD, Alzheimer's disease; UDG, uracil DNA glycosylase.

mutation levels in AD brains have been measured previously, but the results are conflicting. Thus, we measured the mtDNA mutation rate and spectrum in the three experimental groups using the RMC assay, a highly sensitive method that discriminates wild-type from mutated DNA based on the cleavage at a specific restriction site (TaqI) composed of all four canonical nucleotide (5′TCGA3′) (Bielas and Loeb, 2005). This technique allows detection of rare mutations, with the lower detection limit of one mutation per 10^9 bases (Bielas and Loeb, 2005), providing a broader and more complete spectrum of mutations in the samples analyzed.

mtDNA mutation frequency was measured in two different TaqI sites in the human mtDNA genome, at nucleotide positions 1216 and 8006, located at the 12S ribosomal RNA and the MT-COII genes, respectively. The RMC analyses showed that mtDNA mutation frequencies were similar for all three groups, in both brain regions (CE—Fig. 4A; and TC—Fig. 4B). Furthermore, both TaqI sites showed comparable mutation frequencies of around 10-20 mutations per 10^6 base pairs. Similar mutation frequencies have been observed in other studies (Ericson et al., 2012).

3.5. Significant decrease in the mtDNA copy number in TC of AD individuals

As damage accumulation can lead to mtDNA degradation (Shokolenko et al., 2013), we measure mtDNA levels to ascertain whether mtDNA might be a preferential target to degradation in AD. To address this question, ddPCR assays were performed with TaqI-digested DNA and with primers/probe sets targeting mitochondrial (Walker) and nuclear (RPP30) loci (see Supplementary Table 1). For this assay, short amplicons were chosen to make sure that mtDNA damage accumulation would not interfere with amplification during the ddPCR.

Although no variation in mtDNA copy number among the three groups was observed in CE (Fig. 5A), significant mtDNA depletion was observed in TC from AD subjects when compared to controls and hpC (Fig. 5B). Lower mtDNA content in AD subjects was not due to decreased mitochondrial mass, as CS activity and COX4 protein expression levels in whole-brain extracts were similar for all groups (Fig. 5C—E). These results suggest that targeted mtDNA

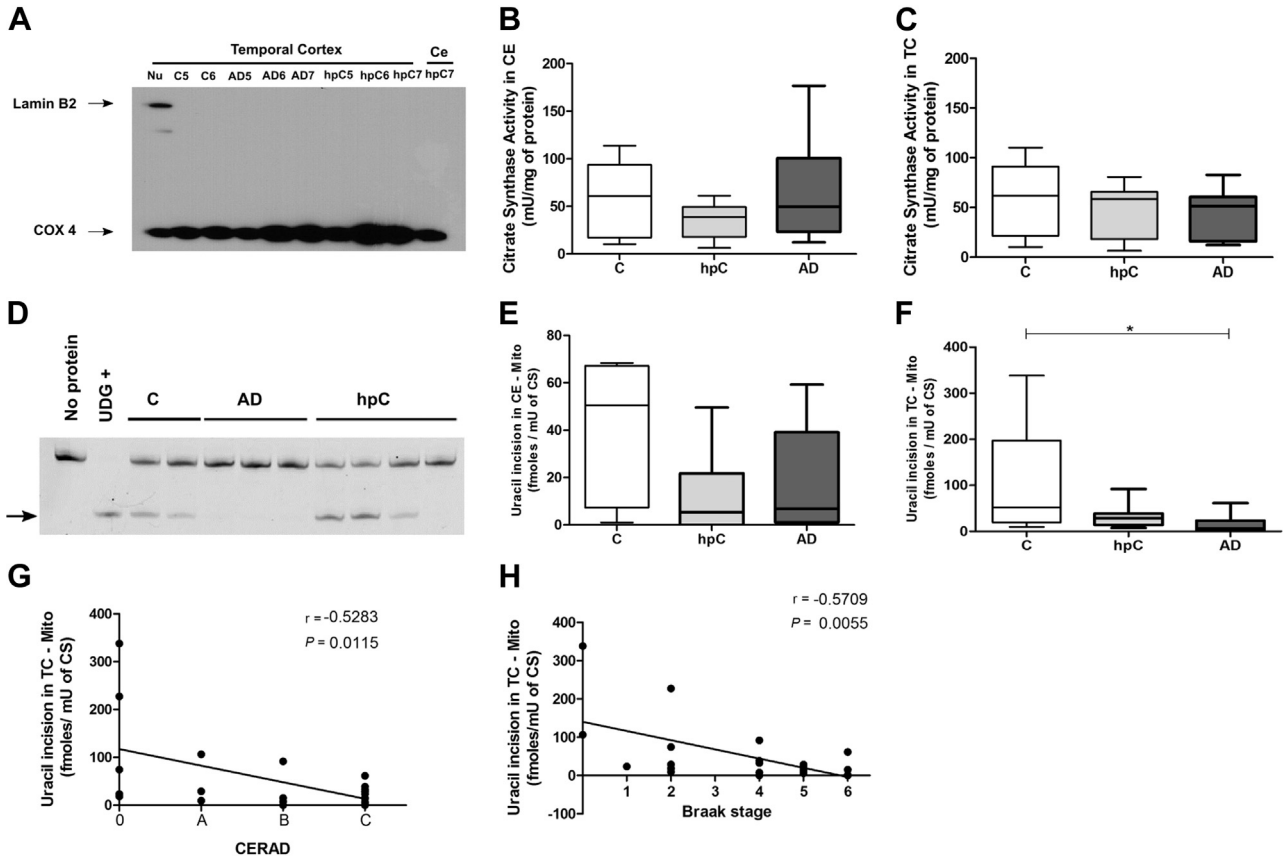

Fig. 2. Lower mitochondrial UDG activity in the AD temporal cortex. Mitochondrial extracts prepared from *postmortem* brains were checked for nuclear contamination by Western blotting against nuclear (Lamin B2) and mitochondrial (COX4) proteins (A). Mitochondrial content in each sample was measured by Citrate Synthase (CS) activity (panels B and C, for CE and TC, respectively). Uracil incision activity was measured as described, and a representative incision gel is presented in (D), using recombinant UDG (UDG+) as a positive control; the migration of the product is indicated by an arrow. Uracil incision was measured in mitochondrial extracts from cerebellum (E) or temporal cortex (F) and normalized to CS activity. Uracil incision activity in TC for each individual was plotted against CERAD score (G) or Braak stage (H). R values represent the Pearson's coefficient and p values <0.05 are considered statistically significant. The incision values presented are mean ± SD of two independent experiments, performed in duplicate (n = 10 per group). * $p < 0.05$. Abbreviations: AD, Alzheimer's disease; UDG, uracil DNA glycosylase.

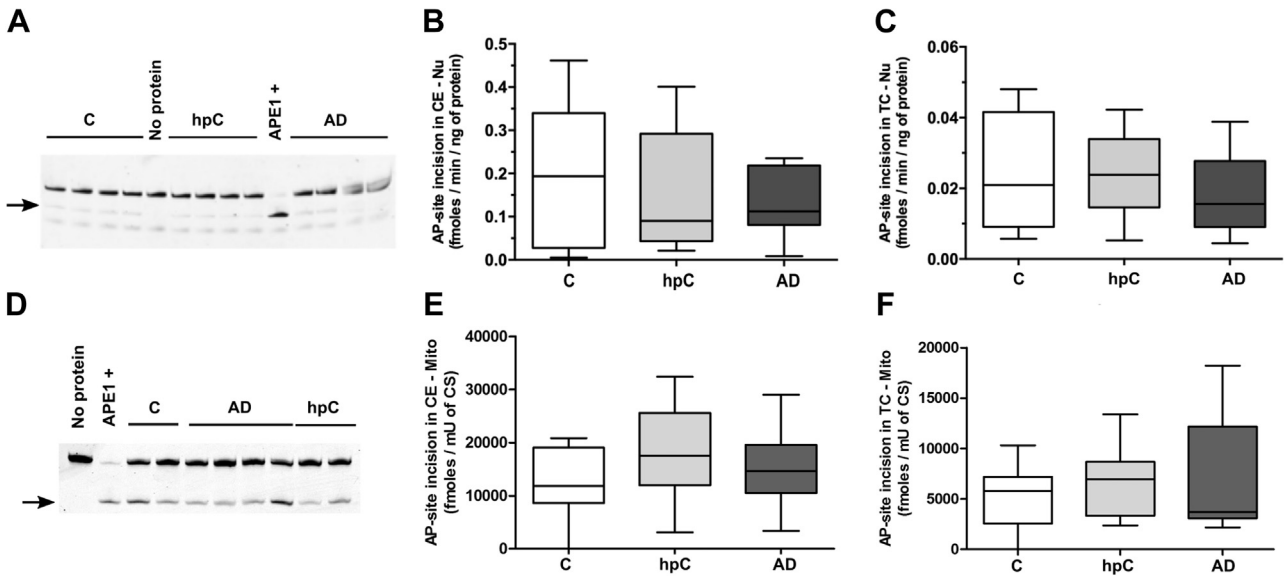

Fig. 3. Nuclear and mitochondrial APE1 activity is not affected in AD. AP-site incision was measured as described and representative incision gels are presented in (A and D), using recombinant APE1 (APE1+) as a positive control. AP incision was measured in CE (B and E) or TC (C and F) nuclear (B and C) and mitochondrial (C and F) extracts. Mitochondrial AP-site incision activity was normalized to CS activity (Fig. 2). The incision values presented are mean ± SD of two independent experiments, performed in duplicate (n = 10 per group). Abbreviations: AD, Alzheimer's disease; hpC, high-pathology control.

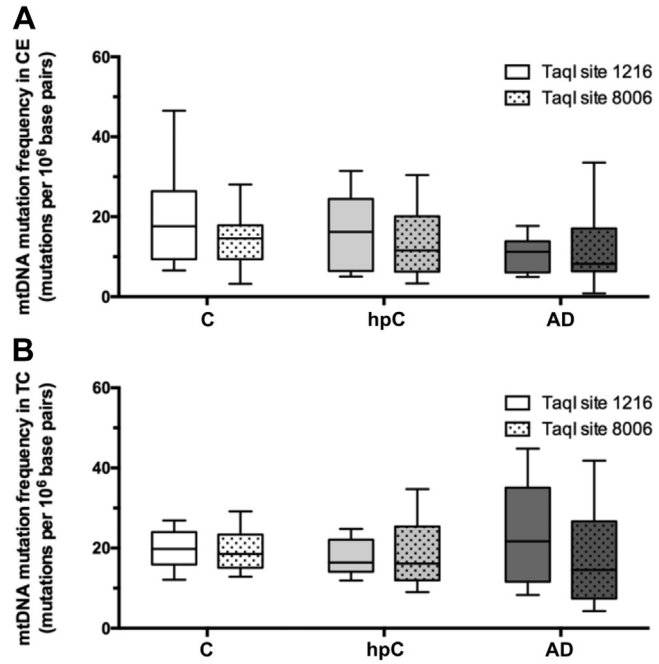

Fig. 4. mtDNA mutation frequency is similar in control, hpC, and AD individuals. Total DNA was isolated from the cerebellum (A) and temporal cortex (B) from all samples (Table 1) and mutation frequency at mtDNA TaqI sites 1216 (clear bars) and 8006 (dotted bars) was analyzed by RMC, as described. The graphs show the mean ± SD of two independent experiments, performed in duplicate (n = 10 per group). Abbreviations: AD, Alzheimer's disease; hpC, high-pathology control; RMC, random mutation capture.

degradation rather than widespread mitophagy may be responsible for this effect. In fact, LC3I/II ratio, an indicative of autophagic flux, was similar in extracts from all three groups (Supplementary Fig. 4).

4. Discussion

Despite great advance in understanding AD pathology, it is still unclear how some of the molecular features of the disease arise and whether they contribute to the pathology. In this regard, it has been postulated that accumulation of mtDNA damage leads to mtDNA mutagenesis and contribute to mitochondrial dysfunction and the clinical outcome (Wallace, 2005). Although the observation that DNA repair activities are impaired in AD brains (Canugovi et al., 2014; Iida et al., 2002; Lovell et al., 2000; Weissman et al., 2007) provided mechanistic support to that, conflicting results regarding mtDNA mutation accumulation in AD have hindered the interpretation of the biological significance of such findings.

Using two different brain regions, an early (TC) and a late (CE) affected region during AD progression, we show that UDG activity is decreased in nuclear and mitochondrial extracts from AD subjects. Interestingly, UDG activity is preserved in hpCs and inversely correlated with both CERAD score and Braak stage, suggesting that it may be a susceptibility factor for disease outcome. Decreased UDG activity and protein levels were found in whole-cell extracts from inferior parietal lobule from AD brains (Weissman et al., 2007). In that study, the authors also observed an inverse correlation between UDG activity and NFTs in brains of amnestic MCI patients, although no correlation was found with Aβ distribution (Weissman et al., 2007). In our samples, however, no changes in UDG protein levels were detected in whole-cell extracts, indicating that other mechanisms might account for decreased UDG activity. UNG2, the nuclear isoform of UDG, has multiple phosphorylation sites within its N-terminal regulatory domain (Hagen et al., 2008; Lu et al., 2004), with the phosphorylated forms displaying higher incision activity on uracil-containing substrates. Moreover, the sequential phosphorylation regulates UNG2 interaction with replication protein A and modulates its activity and turnover (Hagen et al., 2008). One of these phosphorylation sites, Thr^{60}, is a target of the glycogen synthase kinase 3—GSK3 (Baehr et al., 2016), which can be activated by Aβ and in turn promotes Aβ production

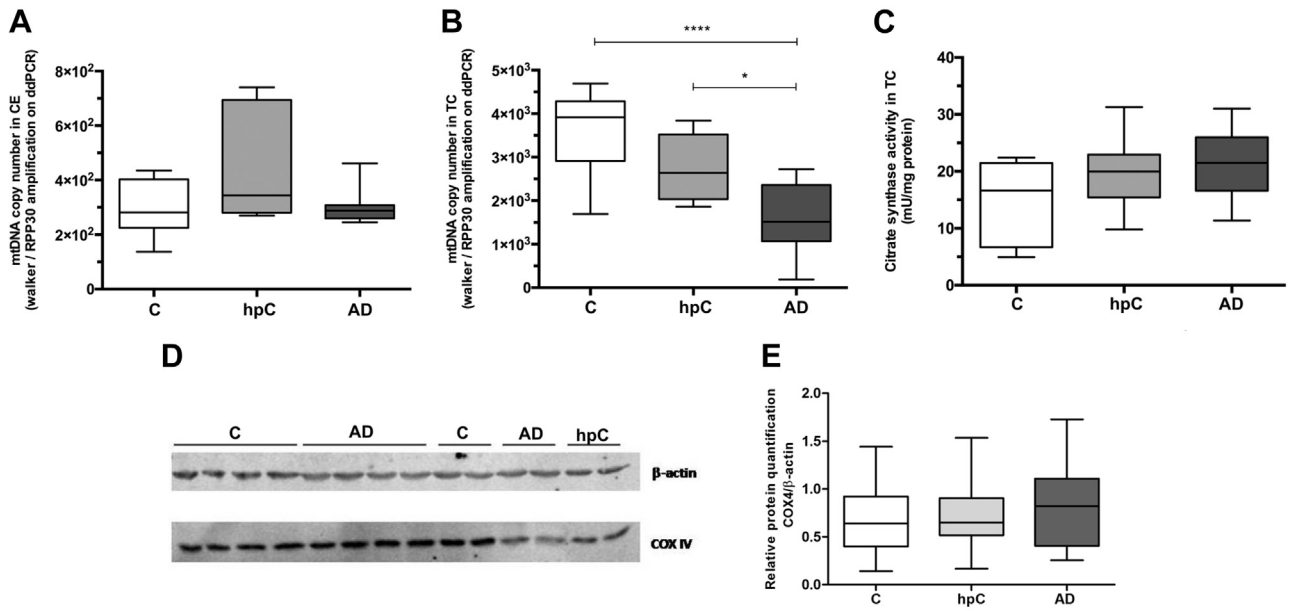

Fig. 5. Lower mtDNA content in AD temporal cortex. mtDNA copy number was measured in total DNA from CE (A) and TC (B) as the ratio of ddPCR amplification of a mitochondrial (Walker site) and a nuclear (RPP30) target. Mitochondrial content in TC whole-cell extract was evaluated by measuring citrate synthase activity (C), as described and COX4 protein levels by Western blotting. A representative blot is presented in panel D; COX4 protein expression was normalized to β-actin expression and quantifications are expressed relative to the control group (E). The values represent the mean ± SD of two independent experiments, performed in duplicate (n = 10 per group). * $p < 0.05$; **** $p < 0.0001$. Abbreviations: AD, Alzheimer's disease; CE, cerebellum; ddPCR, droplet digital PCR; TC, temporal cortex.

(Jope and Johnson, 2004), and is one of the main kinases involved in tau hyperphosphorylation (Ishiguro et al., 1993; Yamaguchi et al., 1996). In addition, Cd(II) ions were shown to inhibit human UDG by displacing catalytic water in the binding pocket, preventing uracil excision (Gokey et al., 2016), and high concentration of this metal ion in blood is associated with AD mortality (Min and Min, 2016) and negatively correlated with tangles in AD subjects (Panayi et al., 2002).

UDG plays a pivotal role in neuronal survival and in the cellular responses to oxidative damage. Lack of UDG induces p53-dependent apoptosis in embryonic rat hippocampal neurons; however, the molecular mechanism remains unclear (Kruman et al., 2004). Folic acid deficiency and high plasma homocysteine have been linked to increased risk of AD (Ravaglia et al., 2005; Seshadri et al., 2002). Impaired one-carbon metabolism, due to low folic acid, leads to uracil misincorporation (Fenech, 2010; Hinterberger and Fischer, 2013) and increased sensitivity to Aβ peptide toxicity (Kruman et al., 2002). Moreover, hippocampal neurons from APP mutant mice became more vulnerable to excitotoxicity and DNA damage when maintained in low folic acid conditions, suggesting that DNA damage accumulation is a determinant for neuronal death (Kruman et al., 2002). Lack of UDG exacerbated the effect of a folic acid–deficient diet in the neurodegenerative process (Kronenberg et al., 2008), indicating a causal relationship between uracil removal and the pathophysiology of the disease.

hpC individuals did not show a significant decrease in UDG activity when compared to controls. This group was first described by Katzman et al., 1988 based on neuropathological and cognitive criteria. A recent study comparing four different groups (controls, nondemented with intermediate probability of AD, nondemented with high probability of AD, and AD) reported that AD individuals had a significant reduction in the number of temporal neurons when compared with controls, whereas no significant neuronal loss was observed in intermediate and high probability of AD (Perez-Nievas et al., 2013). Moreover, AD subjects, but not nondemented subjects with high probability of AD, showed a significant decrease in a component of postsynaptic density (PSD-95) and in a component of presynaptic vesicles (synaptophysin) when compared with controls. The authors suggested that this represents an early synaptic compensatory mechanism that may prevent the cognitive decline (Perez-Nievas et al., 2013).

Although the molecular mechanisms that promote synaptic plasticity are still poorly understood, the mitochondria play a pivotal role in this process. As synaptic transmission requires high levels of ATP and regulation of calcium dynamics, an increased transport of mitochondria to synaptic terminals is required to supply these needs (Mattson and Liu, 2002; Reddy and Beal, 2008). However, intraneuronal accumulation of oligomeric Aβ leads to dysfunctional mitochondrial dynamics and impaired mitochondria anterograde transport, resulting in decreased synaptic function (Calkins et al., 2011). In addition, hippocampal cultured neurons show impaired mitochondrial transport and fragmentation upon exposure to Aβ oligomers (Rui and Zheng, 2016). Thus, the compensatory and protective mechanisms associated with preserved cognitive function in hpC individuals may be related to the functional and morphological integrity of the mitochondria and to its crucial role it plays in synaptic transmission and plasticity.

In line with that, we found that mitochondrial UDG activity was significantly decreased in AD when compared with controls only in TC but not in CE. Our results suggest that mitochondrial UDG may be important in protecting temporal neurons from Aβ toxicity. In fact, HeLa cells exposed to hydrogen peroxide showed a 2.2-fold increase in mitochondrial UDG expression (Akbari et al., 2007), and overexpression of mitochondrial UDG in A549 cells protected from hydrogen peroxide and gossypol toxicity and reduced 8-OHdG levels, indicating that mitochondrial UDG also protects mtDNA from oxidative damage (Liu et al., 2016).

AD individuals harbor more mtDNA lesions than age-matched, cognitively normal individuals (Krishnan et al., 2012; Wang et al., 2005). The higher levels of DNA lesions observed in the mtDNA from AD brains have been attributed to increased oxidative stress (Wang et al., 2014) and lower DNA repair capacity, as shown here and by others (Canugovi et al., 2014; Weissman et al., 2007). DNA lesions can impair mtDNA replication and transcription, whereas lesion bypass by DNA polymerases may result in point mutations, and it has been proposed that increased mtDNA mutagenesis contributes to mitochondrial dysfunction in AD. Previous studies have analyzed the mtDNA mutation spectrum in AD brains (Chang et al., 2000; Chinnery et al., 2001; Coskun et al., 2004; Hoekstra et al., 2016; Lin et al., 2002) but report divergent results as to whether there is a higher mtDNA mutation frequency in AD brains. Using the highly sensitive RMC assay, which can detect even rare and low frequency mutations (Bielas and Loeb, 2005), we found no increased mtDNA mutation frequency in AD brains. A recent study showed that mtDNA point mutation frequency in the hippocampus depends on the disease stage, being significantly elevated in early stage and lower in confirmed AD individuals. The authors suggest that mutated mtDNA may be lost by neuron death during disease progression (Hoekstra et al., 2016). In that study, the group classified as early stage AD had no cognitive decline, Braak stage III or IV, and CERAD score moderate or frequent (Hoekstra et al., 2016), whereas the hpC group used here included only individuals with Braak stages IV or V. Despite the similarities between classification criteria of the groups, some factors may account for the difference in the results, including sample size, the techniques used to quantify the mtDNA mutations, and Braak stage.

Nonetheless, the lower mtDNA copy number detected in AD TC, when compared with hpC and controls, supports the hypothesis that mutated and/or damaged mtDNA may be lost during AD progression. mtDNA depletion could not be attributed to selective mitophagy, as CS activity and COX4 protein levels in whole-brain extracts were similar for all groups. Lower mtDNA copy number was previously reported in Parkinson's (Pyle et al., 2015), Huntington's (Petersen et al., 2014), and also AD (Rice et al., 2014). As proposed by Malik and Czajka, 2013, the mtDNA/nDNA ratio could be taken as a biomarker of mitochondrial dysfunction, as a decreased ratio is observed in several conditions associated with oxidative stress. As mitochondrial content is a consequence of the balance between biogenesis and degradation by mitophagy (Ploumi et al., 2017), similar mitochondrial content is an indicative of normal mitochondrial dynamics and suggests that damaged genomes might be preferentially degraded in AD subjects, rendering mitochondria less efficient and more susceptible to Aβ toxicity.

5. Conclusion

The activity of BER enzyme UDG was significantly decreased in mitochondrial and nuclear extracts of AD TC. Moreover, U-incision inversely correlated with neuropathological hallmarks of AD, suggesting that lower UDG activity is a feature of AD neuropathology and could be a potential biomarker of the development of the disease. Nonetheless, AD individuals did not accumulate more mutations in mtDNA but rather showed lower mtDNA copy number in TC, a region which is subjected to higher NFTs and Aβ stress and therefore should accumulate more DNA damage. Altogether, our results suggest that decreased UDG and BER activity in AD subjects may contribute to DNA damage accumulation, which in turn could lead to degradation of damaged genomes, decreased mtDNA/nDNA ratio and, consequently, mitochondrial dysfunction. As mitochondrial dysfunction was shown to be an early event in several

neurodegenerative disorders (Lin and Beal, 2006), these results provide a better understanding of the molecular mechanism involved in AD neuropathology, establishing factors that may affect the susceptibility and progression of the disease.

Disclosure statement

The authors report no conflicts of interest.

Acknowledgements

The authors thank Felippe Truglio Machado for technical help and all members of the Aging Brain Study Group at the University of São Paulo School of Medicine for tissue processing and case classification.

This work was supported by grants FAPESP/CNPq INCT-Redoxoma [grant number: 08/57,721-3] and FAPESP [grant number: 10/51,906-1] to NCdS-P. DTS was supported by FAPESP post-doctoral fellowship [grant number: 2012/11,889-9] and CNPq [grant number: 150974/2011-6 and 475551/2013-3]. CPMP was supported by a CAPES MSc fellowship [grant number: 33002010017P0].

Appendix A. Supplementary data

Supplementary data associated with this article can be found, in the online version, at https://doi.org/10.1016/j.neurobiolaging.2018.09.015.

References

Akbari, M., Otterlei, M., Pena-Diaz, J., Krokan, H.E., 2007. Different organization of base excision repair of uracil in DNA in nuclei and mitochondria and selective upregulation of mitochondrial uracil-DNA glycosylase after oxidative stress. Neuroscience 145, 1201–1212.

Baehr, C.A., Huntoon, C.J., Hoang, S.M., Jerde, C.R., Karnitz, L.M., 2016. Glycogen synthase kinase 3 (GSK-3)-mediated phosphorylation of uracil N-glycosylase 2 (UNG2) facilitates the repair of floxuridine-induced DNA lesions and promotes cell survival. J. Biol. Chem. 291, 26875–26885.

Bielas, J.H., Loeb, L.A., 2005. Quantification of random genomic mutations. Nat. Methods 2, 285–290.

Braak, H., Braak, E., 1991. Neuropathological stageing of Alzheimer-related changes. Acta Neuropathol. 82, 239–259.

Bradford, M.M., 1976. A rapid and sensitive method for the quantitation of microgram quantities of protein utilizing the principle of protein-dye binding. Anal. Biochem. 72, 248–254.

Calkins, M.J., Manczak, M., Mao, P., Shirendeb, U., Reddy, P.H., 2011. Impaired mitochondrial biogenesis, defective axonal transport of mitochondria, abnormal mitochondrial dynamics and synaptic degeneration in a mouse model of Alzheimer's disease. Hum. Mol. Genet. 20, 4515–4529.

Canugovi, C., Shamanna, R.A., Croteau, D.L., Bohr, V.A., 2014. Base excision DNA repair levels in mitochondrial lysates of Alzheimer's disease. Neurobiol. Aging 35, 1293–1300.

Chang, S.W., Zhang, D., Chung, H.D., Zassenhaus, H.P., 2000. The frequency of point mutations in mitochondrial DNA is elevated in the Alzheimer's brain. Biochem. Biophys. Res. Commun. 273, 203–208.

Chinnery, P.F., Taylor, G.A., Howell, N., Brown, D.T., Parsons, T.J., Turnbull, D.M., 2001. Point mutations of the mtDNA control region in normal and neurodegenerative human brains. Am. J. Hum. Genet. 68, 529–532.

Coskun, P.E., Beal, M.F., Wallace, D.C., 2004. Alzheimer's brains harbor somatic mtDNA control-region mutations that suppress mitochondrial transcription and replication. Proc. Natl. Acad. Sci. U S A 101, 10726–10731.

Eigentler, A., Draxl, A., Wiethüchter, A., Kuznetsov, A.V., Lassing, B., Gnaiger, E., 2015. Laboratory Protocol: Citrate Synthase a Mitochondrial Marker Enzyme. Mitochondr Physiol Network 17.04(03), 1–11.

Ericson, N.G., Kulawiec, M., Vermulst, M., Sheahan, K., O'Sullivan, J., Salk, J.J., Bielas, J.H., 2012. Decreased mitochondrial DNA mutagenesis in human colorectal cancer. PLoS Genet. 8, e1002689.

Fenech, M., 2010. Folate, DNA damage and the aging brain. Mech. Ageing Dev. 131, 236–241.

Gokey, T., Hang, B., Guliaev, A.B., 2016. Cadmium(II) inhibition of human uracil-DNA glycosylase by catalytic water supplantation. Sci. Rep. 6, 39137.

Grinberg, L.T., Ferretti, R.E., Farfel, J.M., Leite, R., Pasqualucci, C.A., Rosemberg, S., Nitrini, R., Saldiva, P.H., Filho, W.J., 2007. Brain bank of the Brazilian aging brain study group - a milestone reached and more than 1,600 collected brains. Cell Tissue Bank. 8, 151–162.

Hagen, L., Kavli, B., Sousa, M.M., Torseth, K., Liabakk, N.B., Sundheim, O., Pena-Diaz, J., Otterlei, M., Horning, O., Jensen, O.N., Krokan, H.E., Slupphaug, G., 2008. Cell cycle-specific UNG2 phosphorylations regulate protein turnover, activity and association with RPA. EMBO J. 27, 51–61.

Hindson, B.J., Ness, K.D., Masquelier, D.A., Belgrader, P., Heredia, N.J., Makarewicz, A.J., Bright, I.J., Lucero, M.Y., Hiddessen, A.L., Legler, T.C., Kitano, T.K., Hodel, M.R., Petersen, J.F., Wyatt, P.W., Steenblock, E.R., Shah, P.H., Bousse, L.J., Troup, C.B., Mellen, J.C., Wittmann, D.K., Erndt, N.G., Cauley, T.H., Koehler, R.T., So, A.P., Dube, S., Rose, K.A., Montesclaros, L., Wang, S., Stumbo, D.P., Hodges, S.P., Romine, S., Milanovich, F.P., White, H.E., Regan, J.F., Karlin-Neumann, G.A., Hindson, C.M., Saxonov, S., Colston, B.W., 2011. High-throughput droplet digital PCR system for absolute quantitation of DNA copy number. Anal. Chem. 83, 8604–8610.

Hinterberger, M., Fischer, P., 2013. Folate and Alzheimer: when time matters. J. Neural Transm. (Vienna) 120, 211–224.

Hoekstra, J.G., Hipp, M.J., Montine, T.J., Kennedy, S.R., 2016. Mitochondrial DNA mutations increase in early stage Alzheimer disease and are inconsistent with oxidative damage. Ann. Neurol. 80, 301–306.

Holloszy, J.O., Oscai, L.B., Don, I.J., Mole, P.A., 1970. Mitochondrial citric acid cycle and related enzymes: adaptive response to exercise. Biochem. Biophys. Res. Commun. 40, 1368–1373.

Iida, T., Furuta, A., Nishioka, K., Nakabeppu, Y., Iwaki, T., 2002. Expression of 8-oxoguanine DNA glycosylase is reduced and associated with neurofibrillary tangles in Alzheimer's disease brain. Acta Neuropathol. 103, 20–25.

Ishiguro, K., Shiratsuchi, A., Sato, S., Omori, A., Arioka, M., Kobayashi, S., Uchida, T., Imahori, K., 1993. Glycogen synthase kinase 3 beta is identical to tau protein kinase I generating several epitopes of paired helical filaments. FEBS Lett. 325, 167–172.

Jope, R.S., Johnson, G.V., 2004. The glamour and gloom of glycogen synthase kinase-3. Trends Biochem. Sci. 29, 95–102.

Jorm, A.F., Jacomb, P.A., 1989. The Informant Questionnaire on Cognitive Decline in the Elderly (IQCODE): socio-demographic correlates, reliability, validity and some norms. Psychol. Med. 19, 1015–1022.

Karahalil, B., Hogue, B.A., de Souza-Pinto, N.C., Bohr, V.A., 2002. Base excision repair capacity in mitochondria and nuclei: tissue-specific variations. FASEB J. 16, 1895–1902.

Katzman, R., Terry, R., DeTeresa, R., Brown, T., Davies, P., Fuld, P., Renbing, X., Peck, A., 1988. Clinical, pathological, and neurochemical changes in dementia: a subgroup with preserved mental status and numerous neocortical plaques. Ann. Neurol. 23, 138–144.

Krishnan, K.J., Ratnaike, T.E., De Gruyter, H.L., Jaros, E., Turnbull, D.M., 2012. Mitochondrial DNA deletions cause the biochemical defect observed in Alzheimer's disease. Neurobiol. Aging 33, 2210–2214.

Krokan, H.E., Otterlei, M., Nilsen, H., Kavli, B., Skorpen, F., Andersen, S., Skjelbred, C., Akbari, M., Aas, P.A., Slupphaug, G., 2001. Properties and functions of human uracil-DNA glycosylase from the UNGgene. Prog. Nucleic Acid Res. Mol. Biol. 68, 365–386.

Kronenberg, G., Harms, C., Sobol, R.W., Cardozo-Pelaez, F., Linhart, H., Winter, B., Balkaya, M., Gertz, K., Gay, S.B., Cox, D., Eckart, S., Ahmadi, M., Juckel, G., Kempermann, G., Hellweg, R., Sohr, R., Hortnagl, H., Wilson, S.H., Jaenisch, R., Endres, M., 2008. Folate deficiency induces neurodegeneration and brain dysfunction in mice lacking uracil DNA glycosylase. J. Neurosci. 28, 7219–7230.

Kruman II, Kumaravel, T.S., Lohani, A., Pedersen, W.A., Cutler, R.G., Kruman, Y., Haughey, N., Lee, J., Evans, M., Mattson, M.P., 2002. Folic acid deficiency and homocysteine impair DNA repair in hippocampal neurons and sensitize them to amyloid toxicity in experimental models of Alzheimer's disease. J. Neurosci. 22, 1752–1762.

Kruman II, Schwartz, E., Kruman, Y., Cutler, R.G., Zhu, X., Greig, N.H., Mattson, M.P., 2004. Suppression of uracil-DNA glycosylase induces neuronal apoptosis. J. Biol. Chem. 279, 43952–43960.

Lin, M.T., Beal, M.F., 2006. Mitochondrial dysfunction and oxidative stress in neurodegenerative diseases. Nature 443, 787–795.

Lin, M.T., Simon, D.K., Ahn, C.H., Kim, L.M., Beal, M.F., 2002. High aggregate burden of somatic mtDNA point mutations in aging and Alzheimer's disease brain. Hum. Mol. Genet. 11, 133–145.

Liu, Z., Hu, Y., Gong, Y., Zhang, W., Liu, C., Wang, Q., Deng, H., 2016. Hydrogen peroxide mediated mitochondrial UNG1-PRDX3 interaction and UNG1 degradation. Free Radic. Biol. Med. 99, 54–62.

Lovell, M.A., Xie, C., Markesbery, W.R., 2000. Decreased base excision repair and increased helicase activity in Alzheimer's disease brain. Brain Res. 855, 116–123.

Lu, X., Bocangel, D., Nannenga, B., Yamaguchi, H., Appella, E., Donehower, L.A., 2004. The p53-induced oncogenic phosphatase PPM1D interacts with uracil DNA glycosylase and suppresses base excision repair. Mol. Cell 15, 621–634.

Malik, A.N., Czajka, A., 2013. Is mitochondrial DNA content a potential biomarker of mitochondrial dysfunction? Mitochondrion 13, 481–492.

Mattson, M.P., 2004. Pathways towards and away from Alzheimer's disease. Nature 430, 631–639.

Mattson, M.P., Liu, D., 2002. Energetics and oxidative stress in synaptic plasticity and neurodegenerative disorders. Neuromolecular Med. 2, 215–231.

Maynard, S., de Souza-Pinto, N.C., Scheibye-Knudsen, M., Bohr, V.A., 2010. Mitochondrial base excision repair assays. Methods 51, 416–425.

Min, J.Y., Min, K.B., 2016. Blood cadmium levels and Alzheimer's disease mortality risk in older US adults. Environ. Health 15, 69.

Mirra, S.S., Heyman, A., McKeel, D., Sumi, S.M., Crain, B.J., Brownlee, L.M., Vogel, F.S., Hughes, J.P., van Belle, G., Berg, L., 1991. The consortium to establish a registry for Alzheimer's disease (CERAD). Part II. Standardization of the neuropathologic assessment of Alzheimer's disease. Neurology 41, 479–486.

Montine, T.J., Phelps, C.H., Beach, T.G., Bigio, E.H., Cairns, N.J., Dickson, D.W., Duyckaerts, C., Frosch, M.P., Masliah, E., Mirra, S.S., Nelson, P.T., Schneider, J.A., Thal, D.R., Trojanowski, J.Q., Vinters, H.V., Hyman, B.T., National Institute on, A., Alzheimer's, A., 2012. National Institute on Aging-Alzheimer's Association guidelines for the neuropathologic assessment of Alzheimer's disease: a practical approach. Acta Neuropathol. 123, 1–11.

Morris, J.C., 1993. The clinical dementia rating (CDR): current version and scoring rules. Neurology 43, 2412–2414.

Panayi, A.E., Spyrou, N.M., Iversen, B.S., White, M.A., Part, P., 2002. Determination of cadmium and zinc in Alzheimer's brain tissue using inductively coupled plasma mass spectrometry. J. Neurol. Sci. 195, 1–10.

Perez-Nievas, B.G., Stein, T.D., Tai, H.C., Dols-Icardo, O., Scotton, T.C., Barroeta-Espar, I., Fernandez-Carballo, L., de Munain, E.L., Perez, J., Marquie, M., Serrano-Pozo, A., Frosch, M.P., Lowe, V., Parisi, J.E., Petersen, R.C., Ikonomovic, M.D., Lopez, O.L., Klunk, W., Hyman, B.T., Gomez-Isla, T., 2013. Dissecting phenotypic traits linked to human resilience to Alzheimer's pathology. Brain 136, 2510–2526.

Petersen, M.H., Budtz-Jorgensen, E., Sorensen, S.A., Nielsen, J.E., Hjermind, L.E., Vinther-Jensen, T., Nielsen, S.M., Norremolle, A., 2014. Reduction in mitochondrial DNA copy number in peripheral leukocytes after onset of Huntington's disease. Mitochondrion 17, 14–21.

Ploumi, C., Daskalaki, I., Tavernarakis, N., 2017. Mitochondrial biogenesis and clearance: a balancing act. FEBS J. 284, 183–195.

Pyle, A., Anugrha, H., Kurzawa-Akanbi, M., Yarnall, A., Burn, D., Hudson, G., 2015. Reduced mitochondrial DNA copy number is a biomarker of Parkinson's disease. Neurobiol. Aging 38, 216.e7–216.e10.

Ravaglia, G., Forti, P., Maioli, F., Martelli, M., Servadei, L., Brunetti, N., Porcellini, E., Licastro, F., 2005. Homocysteine and folate as risk factors for dementia and Alzheimer disease. Am. J. Clin. Nutr. 82, 636–643.

Reddy, P.H., Beal, M.F., 2008. Amyloid beta, mitochondrial dysfunction and synaptic damage: implications for cognitive decline in aging and Alzheimer's disease. Trends Mol. Med. 14, 45–53.

Rice, A.C., Keeney, P.M., Algarzae, N.K., Ladd, A.C., Thomas, R.R., Bennett Jr., J.P., 2014. Mitochondrial DNA copy numbers in pyramidal neurons are decreased and mitochondrial biogenesis transcriptome signaling is disrupted in Alzheimer's disease hippocampi. J. Alzheimers Dis. 40, 319–330.

Robertson, A.B., Klungland, A., Rognes, T., Leiros, I., 2009. DNA repair in mammalian cells: base excision repair: the long and short of it. Cell. Mol. Life Sci. 66, 981–993.

Rui, Y., Zheng, J.Q., 2016. Amyloid beta oligomers elicit mitochondrial transport defects and fragmentation in a time-dependent and pathway-specific manner. Mol. Brain 9, 79.

Seshadri, S., Beiser, A., Selhub, J., Jacques, P.F., Rosenberg, I.H., D'Agostino, R.B., Wilson, P.W., Wolf, P.A., 2002. Plasma homocysteine as a risk factor for dementia and Alzheimer's disease. N. Engl. J. Med. 346, 476–483.

Shokolenko, I.N., Wilson, G.L., Alexeyev, M.F., 2013. Persistent damage induces mitochondrial DNA degradation. DNA Repair (Amst) 12, 488–499.

Soltys, D.T., Pereira, C.P.M., Ishibe, G.N., de Souza-Pinto, N.C., 2015. Effects of post mortem interval and gender in DNA base excision repair activities in rat brains. Mutat. Res. 776, 48–53.

Thompson, P.M., Hayashi, K.M., de Zubicaray, G., Janke, A.L., Rose, S.E., Semple, J., Herman, D., Hong, M.S., Dittmer, S.S., Doddrell, D.M., Toga, A.W., 2003. Dynamics of gray matter loss in Alzheimer's disease. J. Neurosci. 23, 994–1005.

Valente, W.J., Ericson, N.G., Long, A.S., White, P.A., Marchetti, F., Bielas, J.H., 2016. Mitochondrial DNA exhibits resistance to induced point and deletion mutations. Nucleic Acids Res. 44, 8513–8524.

Wallace, D.C., 2005. A mitochondrial paradigm of metabolic and degenerative diseases, aging, and cancer: a dawn for evolutionary medicine. Annu. Rev. Genet. 39, 359–407.

Wang, J., Xiong, S., Xie, C., Markesbery, W.R., Lovell, M.A., 2005. Increased oxidative damage in nuclear and mitochondrial DNA in Alzheimer's disease. J. Neurochem. 93, 953–962.

Wang, X., Wang, W., Li, L., Perry, G., Lee, H.G., Zhu, X., 2014. Oxidative stress and mitochondrial dysfunction in Alzheimer's disease. Biochim. Biophys. Acta 1842, 1240–1247.

Weissman, L., Jo, D.G., Sorensen, M.M., de Souza-Pinto, N.C., Markesbery, W.R., Mattson, M.P., Bohr, V.A., 2007. Defective DNA base excision repair in brain from individuals with Alzheimer's disease and amnestic mild cognitive impairment. Nucleic Acids Res. 35, 5545–5555.

Wilson 3rd, D.M., Bohr, V.A., 2007. The mechanics of base excision repair, and its relationship to aging and disease. DNA Repair (Amst) 6, 544–559.

Wilson 3rd, D.M., Takeshita, M., Grollman, A.P., Demple, B., 1995. Incision activity of human apurinic endonuclease (Ape) at abasic site analogs in DNA. J. Biol. Chem. 270, 16002–16007.

Wright, J.H., Modjeski, K.L., Bielas, J.H., Preston, B.D., Fausto, N., Loeb, L.A., Campbell, J.S., 2011. A random mutation capture assay to detect genomic point mutations in mouse tissue. Nucleic Acids Res. 39, e73.

Yamaguchi, H., Ishiguro, K., Uchida, T., Takashima, A., Lemere, C.A., Imahori, K., 1996. Preferential labeling of Alzheimer neurofibrillary tangles with antisera for tau protein kinase (TPK) I/glycogen synthase kinase-3 beta and cyclin-dependent kinase 5, a component of TPK II. Acta Neuropathol. 92, 232–241.